Bioresource Technology 410 (2024) 131214

Contents lists available at ScienceDirect

Bioresource Technology

journal homepage: www.elsevier.com/locate/biortech

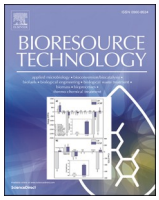

Functional plasticity of HCO_3^- uptake and CO_2 fixation in *Cupriavidus necator* H16

Justin Panich [a,*], Emili Toppari [a], Sara Tejedor-Sanz [a,b], Bonnie Fong [a], Eli Dugan [c], Yan Chen [a], Christopher J. Petzold [a], Zhiying Zhao [d], Yasuo Yoshikuni [a,d,e], David F. Savage [c,f], Steven W. Singer [a]

[a] Biological Systems and Engineering Division, Lawrence Berkeley National Laboratory, Berkeley, CA 94720, USA
[b] Advanced Biofuel and Bioproducts Process Development Unit, Lawrence Berkeley NationalLaboratory, Emeryville, CA 94608, USA
[c] Department of Molecular and Cell Biology, University of California-Berkeley, Berkeley, CA, 94720, USA
[d] The US Department of Energy Joint Genome Institute, Lawrence Berkeley National Laboratory, CA 94720, USA
[e] Environmental Genomics and Systems Biology, Lawrence Berkeley National Laboratory, CA94720, USA
[f] Howard Hughes Medical Institute, University of California, Berkeley, CA 94720, USA

HIGHLIGHTS

- The chassis-independent recombinase-assisted genome engineering (CRAGE) technique is implemented in *C. necator*.
- The role of carbonic anhydrase enzymes for autotrophic metabolism is clarified.
- A suite of dissolved inorganic carbon transporters from *Cyanobacteria* and chemolithotrophic bacteria complement the function of carbonic anhydrase.
- Replacement of HCO_3^- acquisition and CO_2 fixation systems is demonstrated in a single strain.

GRAPHICAL ABSTRACT

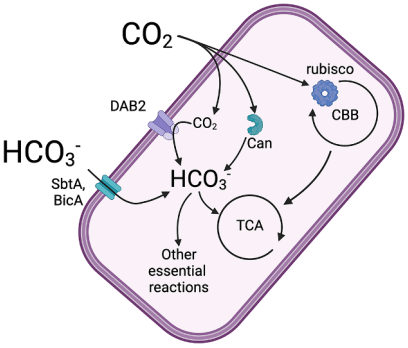

ARTICLE INFO

Keywords:
C1 metabolism
Gas fermentation
Rubisco
Carbonic anhydrase
DAB2
Biomanufacturing
CO_2 conversion
Genome engineering
CRAGE

ABSTRACT

Despite its prominence, the ability to engineer *Cupriavidus necator* H16 for inorganic carbon uptake and fixation is underexplored. We tested the roles of endogenous and heterologous genes on *C. necator* inorganic carbon metabolism. Deletion of β-carbonic anhydrase *can* had the most deleterious effect on *C. necator* autotrophic growth. Replacement of this native uptake system with several classes of dissolved inorganic carbon (DIC) transporters from Cyanobacteria and chemolithoautotrophic bacteria recovered autotrophic growth and supported higher cell densities compared to wild-type (WT) *C. necator* in batch culture. Strains expressing *Halothiobacillus neopolitanus* DAB2 (hnDAB2) and diverse rubisco homologs grew in CO_2 similarly to the wild-type strain. Our experiments suggest that the primary role of carbonic anhydrase during autotrophic growth is to support anaplerotic metabolism, and an array of DIC transporters can complement this function. This work demonstrates flexibility in HCO_3^- uptake and CO_2 fixation in *C. necator*, providing new pathways for CO_2-based biomanufacturing.

* Corresponding author at: Lawrence Berkeley National Laboratory, 1 Cyclotron Rd, Berkeley, CA 94720, USA
E-mail address: justinpanich@lbl.gov (J. Panich).

https://doi.org/10.1016/j.biortech.2024.131214
Received 8 May 2024; Received in revised form 1 August 2024; Accepted 1 August 2024
Available online 9 August 2024

1. Introduction

Society relies on chemical processes that emit vast quantities of CO_2 and other greenhouse gases, contributing substantially to climate change (He and Silliman, 2019; Koch et al., 2013). In 2022, roughly 36.8 billion tons of CO_2 were released into the atmosphere from transportation and heavy industry (Liu et al., 2023; OECD, 2023). Rapid innovation is needed to establish sustainable commodity chemical production at an industrial scale to mitigate climate change caused by greenhouse gas emissions. An attractive strategy is to use gas feedstocks, such as CO_2, CO, CH_4, and H_2, for the biological synthesis of economically crucial chemicals, such as fuels and platform chemicals. These feedstocks offer several advantages: abundance, potential capture from industrial point sources (e.g., ethanol plants, cement factories, steel mills), and generation through electrolysis. The realization of a "C1-based" commodity chemical industry, reliant on one-carbon feedstocks, would mitigate climate change while stimulating economic activity.

Cupriavidus necator H16 (formerly *Ralstonia eutropha* H16) is a well-characterized model organism for C1-based biological conversion due to its ability to grow on CO_2/H_2 or formate as sole carbon and energy sources (Calvey et al., 2023; Panich et al., 2021; Sohn et al., 2021). CO_2 enters the cell via passive diffusion, where it is converted to dissolved inorganic carbon (DIC; HCO_3^-, H_2CO_3) through the action of cytosolic carbonic anhydrases (CAs). These metalloenzymes interconvert CO_2 and soluble HCO_3^-, and are essential in most organisms because HCO_3^- is a cofactor for several reactions in the tricarboxylic acid cycle (e.g. phosphoenolpyruvate carboxylase, carbamoyl phosphate synthetase, 5-amino-imidazole ribotide carboxylase, and biotin carboxylase) (Hashimoto and Kato, 2003; Kusian et al., 2002; Merlin et al., 2003; Mitsuhashi et al., 2004). While CO_2 spontaneously hydrates to HCO_3^- at physiological pH, the HCO_3^- flux requirements are not satisfied by uncatalyzed CO_2 hydration.

CO_2 can also be fixed by *C. necator* through the action of ribulose-1,5-bisphosphate carboxylase/oxygenase (rubisco) to generate biomass using the Calvin-Benson-Bassham (CBB) cycle. Rubisco is a relatively slow enzyme (k_{cat} values for CO_2 are usually 1–22 s^{-1}) and catalyzes an off-target reaction with oxygen, producing a toxic intermediate 2-phosphoglycolate, which must be salvaged (Claassens et al., 2020; Davidi et al., 2020; Flamholz et al., 2019). Carbon fixed from the CBB cycle can be diverted to create sustainable bioproducts using metabolic engineering. *C. necator* has recently been engineered to produce 1,3-butanediol, trehalose, 3-hydroxypropionate, myo-inositol, sucrose, glucose, sesquiterpenes, modified polyhydroxyalkanoates, and lipochitooligosaccharides using CO_2 feedstocks (Gascoyne et al., 2021; Löwe et al., 2021; Milker and Holtmann, 2021; Milker et al., 2021; Nangle et al., 2020; Salinas et al., 2022; Wang et al., 2023, 2022). While this organism has proven useful for CO_2 bioconversion, it has never been fully optimized and typically yields low titers of target molecules (often < 1 g/L) while requiring > 5 % CO_2 (Claassens et al., 2020; Yu and Munasinghe, 2018).

C. necator encodes four carbonic anhydrases (*caa, can, can2, cag*) whose function and relevance to autotrophy remain poorly characterized. *C. necator* also has a cytosolic rubisco with a relatively high specificity for CO_2 ($S_{c/o} = 75$), albeit with a slower rate of catalysis compared to typical cyanobacterial rubiscos ($k_{cat} = 3.8$ s^{-1}) (Gai et al., 2014; Horken and Tabita, 1999; Satagopan and Tabita, 2016; Zhou and Whitney, 2019). In contrast, Cyanobacteria and some chemolithotrophic bacteria have evolved sophisticated CO_2 acquisition and utilization mechanisms, known as "CO_2 Concentrating Mechanisms" (CCMs), enabling robust growth in ambient CO_2 (Espie and Kimber, 2011; Mangan et al., 2016; Flamholz et al., 2020). Bacteria with CCMs acquire CO_2 in the form of HCO_3^- using DIC transporters, a group of evolutionarily diverse membrane transporters that accumulate HCO_3^- in the cytoplasm. HCO_3^- then diffuses into a proteinaceous bacterial microcompartment, the carboxysome, where internalized CAs convert the HCO_3^- to CO_2 near the rubisco active site. The high local concentration of CO_2 facilitates on-target rubisco carboxylation, diminishes oxygenation activity, and avoids the accumulation of the toxic intermediate 2-phosphoglycolate.

Five types of DIC transporters have been characterized to date. BCT1-like complexes use ATP to energize bicarbonate transport (Omata et al., 2002). Other DIC transporters are Na^+/HCO_3^- symporters, such as SbtA and BicA (Fang et al., 2021; Wang et al., 2019a). CUP transporters are thylakoid membrane-associated multi-subunit complexes thought to convert H_2O+CO_2 into HCO_3^- and a proton in alkaline conditions (Han et al., 2017). The fifth class of DIC transporter, the DAB complex (DABs Accumulate Bicarbonate), is a heterodimeric protein thought to convert CO_2 to HCO_3^- on the cytoplasmic face of the cellular membrane using a proton gradient. DABs have been recently shown to function as the predominant DIC accumulation mechanism in *H. neopolitanus* (Desmarais et al., 2019). To date, DABs have been identified in 17 phyla in *Bacteria* and *Archaea* using bioinformatic analysis and have been described for diverse organisms such as *Staphylococcus aureus, Hydrogenovibrio crunogenus,* and in heterotrophic pathogens such as *Bacillus anthracis* and *Vibrio cholera* (Desmarais et al., 2019; Fan et al., 2021; Mangiapia et al., 2017; Scott et al., 2019).

We have previously demonstrated that the robustness of autotrophic growth in three different microbes is co-limited by CO_2 and HCO_3^- availability (Flamholz et al., 2022; Hines et al., 2021). In the current study, we expand upon these findings by elucidating the individual contributions of each of the four carbonic anhydrases in *C. necator*. We show that many DIC transporters can effectively replace CAs during autotrophic metabolism. We conclude that a significant limitation for autotrophic growth in *C. necator* is HCO_3^- availability.

2. Materials and methods

Genetic manipulation and strain storage.

Cloning fragments were amplified with Phusion® High-Fidelity DNA Polymerase (NEB, Ipswich, MA, USA) or Q5® High-Fidelity DNA Polymerase (NEB, Ipswich, MA, USA). PCR products were digested with Dpn1 (NEB, Ipswich, MA, USA) to destroy the original template and were purified using the QIAquick Gel Extraction Kit (Qiagen, Hilden, Germany). Ligation and assembly of DNA fragments were performed with NEBuilder® HiFi DNA Assembly Master Mix (NEB, Ipswich, MA, USA) according to the manufacturer's protocol. Transformations were carried out via heat shock ($CaCl_2$ method) into *E. coli* S17-1 cells. Cloned plasmids were purified using the QIAprep Spin Miniprep Kit (Qiagen, Hilden, Germany). Whole plasmid sequencing was performed by Plasmidsaurus (Arcadia, CA).

Plasmid pW5Y::ara-dab2 was assembled using the yeast recombination plasmid assembly technique (Kuijpers et al. 2013). Briefly, a 5840 bp fragment from pbadt::hnDAB2 encoding the *araC* induction system and hneap_0212 and hneap_0211 encoding the hnDAB2 operon driven by the P_{BAD} promoter was PCR amplified with 60 bp overlaps to the pW5Y backbone. The pW5Y backbone was amplified in two fragments, each ~ 6000 bp. The three fragments were gel purified and were transformed in yeast cells made competent using the Frozen EZ Yeast Transformation II kit® (Zymo Research, Orange, CA, USA). Transformants were selected for on CSM-Ura plates. Plasmids were purified using the Zymoprep Yeast Plasmid Miniprep II kit® (Zymo Research, Orange, CA, USA). Plasmids were then sequenced using the Plasmidsaurus (Arcadia, CA) large plasmid sequencing service.

C. necator H16 was routinely grown in LB media for cultivation and genetic procedures. Genomic deletions were made using a Kanamycin-SacB counterselection scheme using the suicide vector pKD18, and were performed by conjugation between plasmid-carrying *E. coli* S-17 strains and selected *C. necator H16* strains on LB agar plates and incubated overnight at 30 °C. Conjugate cells were isolated on LB agar plates in the presence of 300 ng/mL kanamycin and 40 ng/mL gentamicin and incubated until *C. necator* colonies were observed. Mutations were

verified using colony PCR using primers flanking each genomic deletion site. Mutants were then isolated for single colonies three times on LB agar and were verified again using colony PCR to ensure the stability of genome modifications. To create HCR strains, such as Δ*can*, plates were incubated in plastic gas bags containing saturating CO_2 at 30° C. For strain storage, cells were inoculated into LB medium with appropriate antibiotics and were incubated overnight. Cells were pelleted to concentrate the biomass and were resuspended in 15 % (v/v) glycerol, placed in cryogenic tubes, and stored at −80 °C. All strains and plasmids used in this study are shown in Table 1 and Table 2.

Chassis-independent Recombinase Assisted Genome Engineering (CRAGE) method for C. necator H16.

The CRAGE method was carried out as previously described, with modifications described in the SI(Wang et al., 2019b). Briefly, the plasmid encoding the mariner-based transposon harboring the landing pad (pW17) was modified to remove Cre recombinase and T7 RNA polymerase from plasmid pW17′_noCreReg, and selection of the altered landing pad was carried out by conjugation into strain JP2281 (Δ*caa*Δ*can*Δ*cbbLS*1Δ*cbbLSp*), followed by selecting for growth on 200 μg/mL kanamycin in saturating CO_2. PacBio sequencing was carried out at the Joint Genome Institute in Berkeley, CA, to identify the landing pad location in 16S rRNA (5′ CCAGCTACTGATCGTCGCCTTGGTAGGCTTT-TACCCCACCAACTA::landing_pad:: TAGCTAATCAGACATCGGCCGCCC TGTAGCGCGAGGCCTTGC 3′). DAB2 was assembled into pW5Y under the *araBAD* promoter using yeast recombination cloning and was sequenced by the DIVA team at the Agile BioFoundry (Iizasa and Nagano, 2006; van Leeuwen et al., 2015). pW5Y.DAB2 was then conjugated into strain (JP2415 *C. necator* Δ*caa*Δ*can*Δ*cbbLS*2Δ*cbbLSp LP3*), and recombinants with DAB2 in the chromosome were selected for by growth on LB plates with no antibiotics in ambient air.

Autotrophic growth in batch culture.

C. necator strains were incubated overnight in 5 mL LB containing 200 μg/mL kanamycin (to retain plasmids) in 20 mL crimp-top tubes, supplemented with 10 % CO_2. Cultures were washed three times in Cupriavidus Minimal Media (CMM) and were inoculated into 150 mL serum vials in 5 mL of CMM without a carbon source. The vials were sealed and vacuumed. Gasses were transferred from gas sampling bags using syringes and needles with 62 % H_2 and 10 % O_2, and indicated partial pressures of CO_2. Cells were grown at 30 °C at 200 RPM for 48 h and were then measured for terminal OD_{600} using a Molecular Devices® SpectraMax M2 spectrophotometer using a cuvette with a 1 cm path length. The CMM contained 4.614 g/L Na_2HPO_4, 4.019 g/L NaH_2PO_4, 1.0 g/L NH_4Cl, 0.455 g/L $MgSO_4*H_2O$, 0.453 g/L K_2SO_4, 0.047 g/L $CaCl_2$, and 1 mL/L trace minerals solution (0.48 g/L $CuSO_4*5H_2O$, 2.4 g/L $ZnSO_4*7H_2O$, 2.4 g/L $MnSO_4*H_2O$, 15 g/L $FeSO_4*7H_2O$). The media was adjusted to pH=6.8. The media was supplemented with 100 μg/mL kanamycin for experiments requiring the retention of pbadt-derived plasmids. Plasmids were not induced with L-arabinose for any of the experiments reported here, as we found basal expression rates of DIC transporters and CAs to be sufficient for function using pbadt vectors. However, L-arabinose (0.02 %) was added to cultures to express hnDAB2 from the chromosome in rubisco swapping experiments at the initiation of batch autotrophic growth.

Table 1
Strains used in this study.

Strain number	Genotype	Description
JBx_257052	*C. necator* H16 Δ*A0006*	Wild-type C. necator H16 modified for high-efficiency electroporation
JBx_257053	Δ*caa*Δ*can*	Defective for two most important CA's; HCR phenotype
JBx_257054	Δ*caa*	no HCR phenotype
JBx_257055	Δ*can*	HCR phenotype
JBx_257056	Δ*can2*	no HCR phenotype
JBx_257057	Δ*cag*	no HCR phenotype
JBx_257058	Δ*caa*Δ*can*Δ*cag*Δ*can2*	Defective for all CA's, has HCR phenotype
JBx_257059	Δ*caa*Δ*can*Δ*cbbLS*2Δ*cbbLSp Ralstonia*	Strain JBx_257053 with both copies of cbbLS knocked out
JBx_257060	*C. necator* Δ*caa*Δ*can*Δ*cbbLS*2Δ*cbbLSp LP3*	Strain JBx_257059 with CRAGE landing pad in rpsL gene
JBx_257061	Δ*caa*Δ*can*Δ*cbbLSp*Δ*cbbLSc1 LP3::dab2*	Strain JBx_257060 with DAB2 integrated; grows in ambient air

Table 2
Plasmids used in this study.

Part number	Plasmid name	Description
JBx_023820	pbadt::RFP	RFP under arabinose-inducible promoter
JBx_257062	pbadt::hnDAB2	DAB2 from *H. neopolitanus* in pbadt backbone
JBx_257063	pbadt::sbtA	SbtA from *Synochococcus elongatus* PCC6301 in pbadt backbone (checking which host its from)
JBx_257064	pbadt::bicA	BicA from *Synechococcus* spp. PCC7002 in pbadt backbone
JBx_257065	pbadt::afDAB2	DAB2 from *Acidothiobacillus ferrooxidans* in pbadt backbone
JBx_257066	pbadt::vcDAB2	DAB2 from *Vibrio cholera* in pbadt backbone
JBx_257067	pbadt::baDAB2	DAB2 from Bacillus anthracis in pbadt backbone
JBx_257068	pabdt::hnDAB1	DAB1 from Halothiobacillus neopolitanus in pbadt backbone
JBx_257069	pbadt::fmDAB2	DAB2 from *Ferrovum myxofaciens* in pbadt backbone
JBx_257071	pw17::kmNoCre	minimal landing pad for CRAGE on tn5, for transposition
JBx_257072	pW5Y	backbone for CRAGE target assembly
JBx_257073	pW5Y::araC-dab2	DAB2 from *H. neopolitanus* in with araC-P_{BAD} promoter
JBx_257074	pCbb::gallionella	rubisco from *Gallionella* sp. under H16 Cbb promoter
JBx_257075	pCbb::rubrum	rubisco from *R. rubrum* under H16 Cbb promoter
JBx_257076	pCbb::sphaeroides	rubisco from *R. sphaeroides* under H16 Cbb promoter
JBx_257077	pCbb::6301	rubisco from PCC 6301 under H16 Cbb promoter
JBx_258159	pbadt::can	Can carbonic anhydrase from *C. necator* in pbadt
JBx_258160	pbadt::caa	Caa carbonic anhydrase from *C. necator* in pbadt

Autotrophic growth in gas bioreactors.

Cells were pre-cultured autotrophically in batch with 20 mL CMM containing 100 μg/mL kanamycin with 130 mL headspace containing 62 % H_2, 10 % O_2, and 10 % CO_2 balanced with N_2, grown at 30 °C with 200 RPM shaking for 48 h. Growth of strains in bioreactors was performed using a bioXplorer® 400P system (HEL Ltd, UK) and WinIso® software for online monitoring and control. Each bioreactor was equipped with pH, dissolved oxygen (DO), temperature, and pressure controllers. The pH was controlled automatically using software provided by HEL using the default setting and was performed by titration of 14 % NH_4OH with a set point of pH=6.7. The reactors were sterilized in an autoclave (120 °C, 30 min), and filtered-sterilized autotrophic medium with kanamycin (100 μg mL^{-1}) was batched into each. Temperature was maintained at 30 °C and agitation at 1000 rpm. The initial OD_{600} for all bioreactor experiments was between 0.05 and 0.10.

Experiments for growth in ambient air (i.e. Fig. 5A) were performed with H_2 (5 %) (99.999 % purity, Linde, US) and air (95 %) continuously fed employing gas mass flow controllers and a total gas flow of 150 mL*min^{-1}. The total working volume of the reactors was 300 mL.

Experiments using high CO_2 levels were conducted with either 5 % CO_2 with 10 % O_2 and 85 % H_2 (i.e. Fig. 5B), or 10 % CO_2 and variable O_2, with a starting flow of 3.5 % O_2 and 86.5 % H_2 (i.e. Fig. 5C). The total flow was 200 mL*min^{-1}, and the reactor's net volume was 250 mL. Oxygen flow was adjusted as consumed to maintain dissolved oxygen saturation levels under 30 % to minimize any possible inhibition of autotrophic growth. Growth was measured by regularly sampling 2 mL

of medium and analyzing optical density with a spectrophotometer in 10 mm pathlength cuvettes.

Heterotrophic growth assay of CA defective and complemented strains.

Cells were grown overnight at 30° C and 200 RPM in 6 mL of LB media supplemented with 200 μg mL^{-1} kanamycin in 20 mL crimp cap tubes supplemented with 10 % CO_2. Cells were pelleted and washed three times in CMM and were added to a 96-well flat-bottom plate (Thermo Scientific, USA, Cat #167008) in CMM media containing 1 % fructose and 200 μg mL^{-1} kanamycin to $OD_{600} = 0.04–0.05$ as measured in a BioTek Synergy H1 Multimode plate reader (Agilent, Santa Clara, CA, USA) set to 30° C. The plate was read for 68.5 h, recording OD_{600} in ten-minute intervals after a programmed five-second gentle shake.

Proteomics analysis.

C. necator autotrophic cultures were collected at 48 h of growth at 30 °C and 200 RPM in 150 mL seared serum bottles containing 5 mL of microbial culture in 62 % H_2, 10 % O_2, and indicated concentrations of CO_2. Cells were harvested and stored at −80 °C until further processing. Protein was extracted from cell pellets, and tryptic peptides were prepared by following the established proteomic sample preparation protocol (Chen et al., 2023). Briefly, cell pellets were resuspended in Qiagen P2 Lysis Buffer (Qiagen, Germany) to promote cell lysis. Proteins were precipitated with the addition of 1 mM NaCl and 4 x vol acetone, followed by two additional washes with 80 % acetone in water. The recovered protein pellet was homogenized by pipetting mixing with 100 mM ammonium bicarbonate in 20 % methanol. Protein concentration was determined by the DC protein assay (BioRad, USA). Protein reduction was accomplished using 5 mM tris 2-(carboxyethyl)phosphine (TCEP) for 30 min at room temperature, and alkylation was performed with 10 mM iodoacetamide (IAM; final concentration) for 30 min at room temperature in the dark. Overnight digestion with trypsin was accomplished with a 1:50 trypsin:total protein ratio. The resulting peptide samples were analyzed on an Agilent 1290 UHPLC system coupled to a Thermo Scientific Orbitrap Exploris 480 mass spectrometer for discovery proteomics (Chen et al., 2022). Briefly, peptide samples were loaded onto an Ascentis® ES-C18 Column (Sigma–Aldrich, USA) and were eluted from the column by using a 10-minute gradient from 98 % solvent A (0.1 % FA in H2O) and 2 % solvent B (0.1 % FA in ACN) to 65 % solvent A and 35 % solvent B. Eluting peptides were introduced to the mass spectrometer operating in positive-ion mode and were measured in data-independent acquisition (DIA) mode with a duty cycle of 3 survey scans from *m/z* 380 to *m/z* 985 and 45 MS2 scans with precursor isolation width of 13.5 *m/z* to cover the mass range. DIA raw data files were analyzed by an integrated software suite DIA-NN (Demichev et al., 2020). The databases used in the DIA-NN search (library-free mode) are *E. coli* and *C. necator* latest Uniprot proteome FASTA sequences plus the protein sequences of the heterologous proteins and common proteomic contaminants. DIA-NN determines mass tolerances automatically based on first-pass analysis of the samples with automated determination of optimal mass accuracies. The retention time extraction window was determined individually for all MS runs analyzed via the automated optimization procedure implemented in DIA-NN. Protein inference was enabled, and the quantification strategy was set to Robust LC=High Accuracy. Output main DIA-NN reports were filtered with a global FDR=0.01 on both the precursor level and protein group level. The Top3 method, which is the average MS signal response of the three most intense tryptic peptides of each identified protein, was used to plot the quantity of the targeted proteins in the samples (Ahrné et al., 2013; Silva et al., 2006).

The generated mass spectrometry proteomics data have been deposited to the ProteomeXchange Consortium via the PRIDE partner repository with the dataset identifier PXD051976 (Perez-Riverol et al., 2022)

3. Results and discussion

Can and Caa are the most relevant CAs for autotrophic growth in C. necator.

Prior studies have interrogated the function of each of the four carbonic anhydrases found in the *C. necator* genome during heterotrophic and autotrophic growth (Gai et al., 2014; Kusian et al., 2002). In agreement with previously published studies, a high CO_2 requiring (HCR) phenotype occurred during routine cultivation when *can* was deleted. Individual deletions of *caa, can2,* or *cag* did not significantly affect heterotrophic growth in ambient air. Deletion of all four carbonic anhydrases (Δ*caa*Δ*can*Δ*cag*Δ*can2*) had the same phenotypic effect as the Δ*can* mutant.

We next examined the growth of individual knockouts and the quadruple knockout in autotrophic growth conditions in increasing CO_2 partial pressures (0.05 %, 0.5 %, 1.5 %, and 5 % CO_2) by measuring the OD_{600} of each culture after 48 h of autotrophic growth in sealed flasks, with cultures inoculated at an $OD_{600} = 0.10$ from heterotrophic precultures. Growth was poor for all strains at 0.05 % CO_2, likely because the cells consume the CO_2 in the sealed flasks before appreciable growth occurs. The Δ*can2* and Δ*cag* strains grew to a similar endpoint as the WT strain. The Δ*can* strain showed an apparent growth defect at 0.5 % CO_2 and higher and also exhibited decreased turbidity at 0.05 % CO_2 after 48 h of incubation. Similarly, deletion of *caa* caused only a minor growth defect but showed robust growth at 1.5 % CO_2 (Fig. 1A). We observed a statistically significant decrease in OD_{600} in the ΔΔ*caa* mutant at 5 % CO_2 relative to 1.5 % CO_2. Since Caa has been reported to localize to the periplasm, Caa may have a role in local pH regulation affecting the proton gradient or transport systems. In its absence, cells may suffer from pH imbalance in the periplasm in high CO_2 partial pressures, manifesting in an apparent growth defect. To confirm the role of Can for autotrophic growth, we complemented the Δ*caa*Δ*can* and Δ*caa*Δ*can*Δ*can2*Δ*cag* strains with a Can plasmid and found that the expression of Can is sufficient to support autotrophic growth in both strains (Fig. 1B). Our results indicate that Can is the primary CA involved in heterotrophic and autotrophic growth of *C. necator* H16, a conclusion that is supported by multiple lines of published research (Claassens et al., 2020; Kusian et al., 2002). The Caa enzyme has been proposed as a second CA involved in DIC metabolism in *C. necator*; however, we found only minor effects on growth in *caa* deletion mutants (Gai et al., 2014).

A suite of dissolved inorganic carbon transporters promotes C. necator autotrophic growth.

To assess the functionality of each DIC transporter in *C. necator*, we chose a strain lacking the two most essential CAs for autotrophic growth (Δ*can*Δ*caa*). We assessed the performance of six DAB-type transporters, a SbtA homolog from *Synechococcus elongatus* PCC 6301, and a BicA homolog from *Synechococcus* sp. PCC 7002(Gupta et al., 2020; Shibata et al., 2002). The expression of DAB2 from *H. neopolitanus* (hnDAB2) showed comparable growth to WT cells at lower CO_2 partial pressures (0.05 % and 0.5 % CO_2). However, growth surpassed WT in CO_2 in high partial pressures of CO_2 (1.5 % and 5 %) (Fig. 2A). Proteome analysis does not indicate that the expression of the two remaining CAs was impacted by hnDAB2 expression (Fig. 2B-2D). We also found that hnDAB2 could complement the quadruple knockout strain, eliminating any substantial role for other known CAs in DIC transporter-enabled autotrophic growth (Supplementary Information). Proteomics revealed that rubisco expression is suppressed in 0.05 % CO_2, and 0.5 % CO_2 in the DAB2/Δ*caa*Δ*can* strain relative to WT, but this data is difficult to interpret because recent work has shown that expression of rubisco is not a limiting factor in *C. necator* when grown autotrophically (Jahn et al., 2021).

The performance of many DIC transporters was similar: hnDAB2, afDAB2, SbtA, and BicA resulted in endpoint OD_{600} values surpassing WT *C. necator* at 1.5 % and 5 % CO_2 (Fig. 3). The DAB2 homolog from *Ferrovum myxofaciens* also exceeded the growth of WT in 5 % CO_2 but performed worse than WT in 0.05 %-1.5 % CO_2. In contrast, expression of DAB2 homologs from heterotrophic pathogens *Bacillus anthracis* and *Vibrio cholera* in the Δ*caa*Δ*can* background gave poor growth, despite a previous report of high activity for these homologs in a CA-free strain of

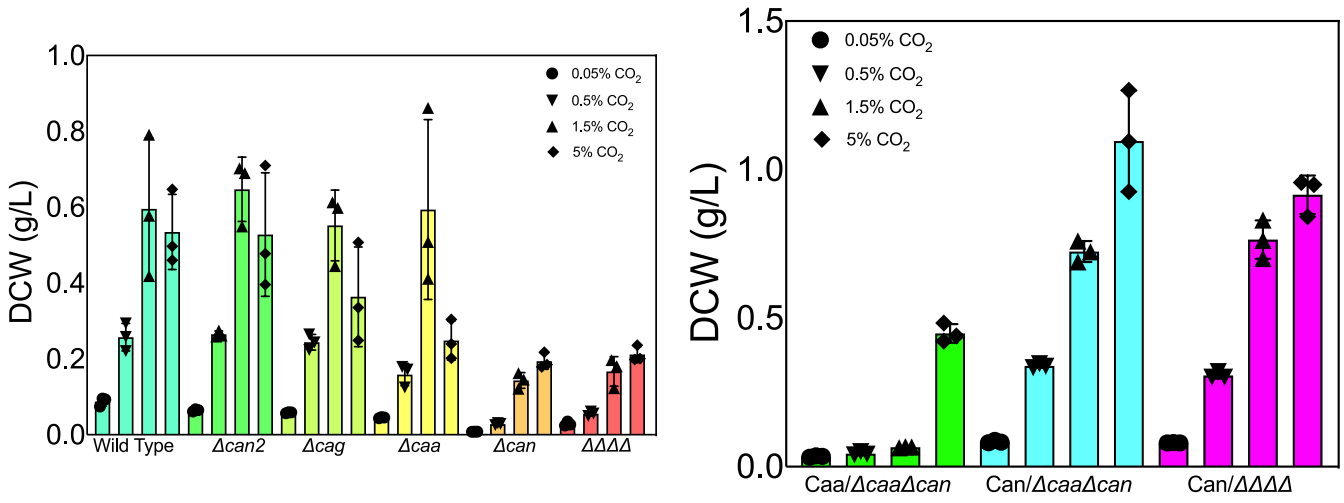

Fig. 1. A. Growth profiles of CA deletion mutants. Terminal OD_{600} at 48 h is shown in 62 % H_2/10 % O_2 and increasing CO_2 partial pressure. Cells were inoculated from heterotrophic cultures at $OD_{600} = 0.1$. B. Can is sufficient for autotrophic growth, while Caa is not sufficient or necessary. Can and Caa were cloned on a pBBR1-MCS-based vector and were introduced into either Δ*caa*Δ*can* or the quadruple CA deletion mutant (ΔΔΔΔ). Cells were inoculated at $OD_{600} = 0.1$ from heterotrophic cultures, and terminal OD_{600} values were measured after 48 hr.

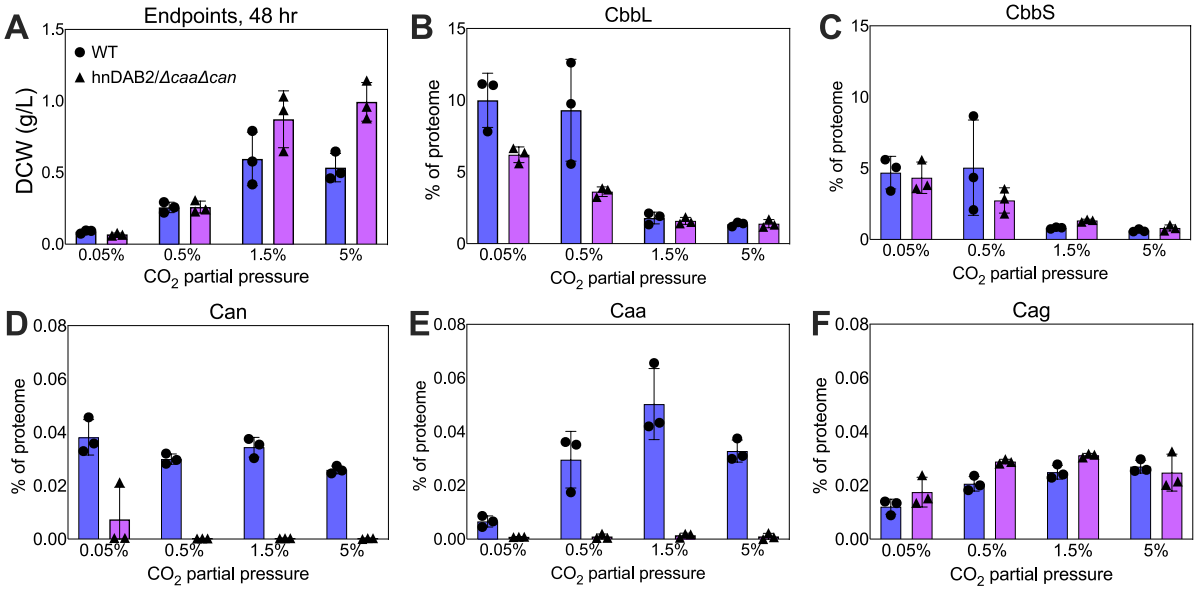

Fig. 2. Comparison of growth characteristics and expression of key enzymes for autotrophy in wild-type and hnDAB2-complemented CA deficient mutant (Δ*caa*Δ*can*). Panel A) Summary of growth data from previous figures of terminal endpoints at 48 hr in autotrophic cultures in WT or hnDAB2/Δ*caa*Δ*can*. Panel B, C) Expression profiles for the large subunit (CbbL) and small subunit (CbbS) of rubisco Panel D) Expression of Caa seems to be influenced by CO_2 partial pressure in WT cells but is knocked out in the hnDAB2-expressing strain. Panel E, F) Cag and Can expression do not seem to be affected by CO_2 partial pressure or expression of hnDAB2. Can2 was not detected in these experiments.

E. coli (Desmarais et al., 2019). Similarly, DAB1 from *H. neapolitanus* failed to rescue the growth of Δ*caa*Δ*can*.

DIC transport suppresses bicarbonate starvation in Δcan strains.

Our experiments demonstrate that several mechanistically distinct DIC transporters can complement strains of *C. necator* that are defective for the native CA Can. Our findings expand on discussions regarding bicarbonate/CO_2 colimitation for autotrophic growth (Flamholz et al., 2022). CO_2 readily diffuses in and out of the cell (permeability coefficient $P_C \approx 0.1–1$ cm/s) (Gutknecht et al., 1977; Hannesschlaeger et al., 2019; Mangan et al., 2016). Consequently, the internal CO_2 concentration is determined almost exclusively by the environmental conditions. At the lowest CO_2 conditions tested (0.05 %), we expect autotrophic growth to be limited by rubisco flux since the *C. necator* rubisco has a $K_{M(CO2)}$ of 66 uM (in the presence of ambient air), corresponding to a CO_2 gas concentration by volume of 0.16 % in the headspace, as calculated by Henry's law (Bowien et al., 1976). The rubisco will be saturated in the 0.5 % CO_2 condition and higher and should not be a growth limitation. In contrast to CO_2, bicarbonate is a charged species that does not readily cross the cellular membrane. In the absence of CAs or DIC transport activity, the cellular flux of bicarbonate via the spontaneous hydration of CO_2 is insufficient to meet the metabolic demands of anaplerosis. Therefore, we attribute the growth defect of Δ*can* to bicarbonate starvation and the subsequent rescue by DAB2, SbtA, and BicA to alleviating the bicarbonate bottleneck, which is also supported by heterotrophic growth experiments showing that hnDAB2 is capable of restoring growth

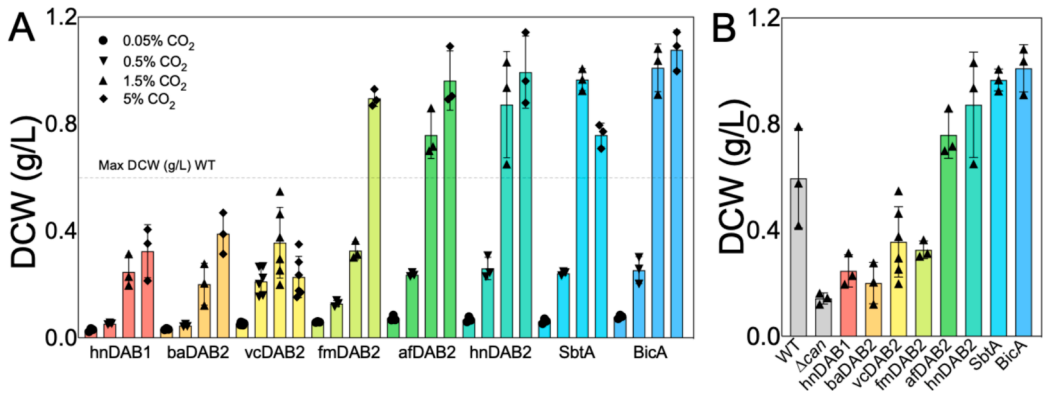

Fig. 3. Performance of heterologous bicarbonate transporters in Δ*caa*Δ*can* (ΔCA). Panel A) Autotrophic endpoints in batch culture were measured after 48 hr of autotrophic growth in 62 % H_2/10 % O_2 and increasing CO_2 partial pressure. The dotted line indicates the terminal OD_{600} of WT *C. necator* at 48 hr in 1.5 % CO_2. Abbreviations: Hn = *Halothiobacillus neopolitans* Ba = *Bacillus anthracis* Vc = *Vibrio cholera* Fm = *Ferrovum myxofaciens* Af = *Acidothiobacillus ferrodoxans* SbtA from *Synechococcus elongatus* PCC 6301, BicA from *Synechococcus* sp. PCC 7002. Panel B) Representative data using the 1.5 % CO_2 partial pressure data from Panel A.

of the CA-defective strain in 1 % fructose (Fig. 4).

Our finding is similar to a recent result in C_3 plants, where a CA defective mutant was fully capable of carrying out photosynthesis and only showed minor effects on the overall growth of the plant (Hines et al., 2021). Our result regarding the importance of DIC accumulation in autotrophic metabolism is also supported by experiments showing that the expression of BicA and SbtA are well-suited to promote high cell density in high CO_2 partial pressures (1.5–5 % CO_2). To our knowledge, this is the first report of functional heterologous expression of BicA, as several BicA homologs failed to rescue the growth of a ΔCA strain of *Escherichia coli* (Du et al., 2014).

The hnDAB2-expressing strain grows similarly to WT in constant-flow bioreactors but underperforms at high CO_2.

We next studied the growth profiles of our strains in constant-flow gas bioreactors under three conditions to assess the industrial relevance of our findings. The hnDAB2/ΔCA strain performed similarly to WT cells in ambient air supplemented with 5 % H_2, while the ΔCA strain did not grow (Fig. 5A). We also tested two bioreactor conditions with CO_2 partial pressures that are saturating for rubisco (5 % and 10 % CO_2 Fig. 5B and 5C, respectively). We found that the WT strain grew much better in elevated CO_2 than the hnDAB2/ΔCA strain.

While strains expressing hnDAB2 outperformed WT in batch cultures at 1.5–5 % CO_2, we saw the opposite trend in constant-flow bioreactors. Given the robustness of the batch culture results, the bioreactor results were initially perplexing to us. The differences in equilibria between CO_2 and HCO_3^- in these two systems should be considered. In batch culture, we would expect that the majority of inorganic carbon is in the form of HCO_3^- because mass transfer can occur over a prolonged period of time, and the equilibrium heavily favors HCO_3^- formation. In contrast, the bioreactor flowed gaseous CO_2 continuously, effectively giving a much higher concentration of gaseous CO_2 compared to batch culture conditions. DAB2 is thought to work by hydrating CO_2 on the cytoplasmic face of the complex by utilizing protons from the proton motive force (PMF). Given this mechanism, hnDAB2 may consume a large portion of the PMF in the higher concentrations of CO_2 in the bioreactor, imparting a growth disadvantage relative to WT cells expressing Can CA, which produces bicarbonate from CO_2 without consuming significant cellular resources such as PMF, ATP, or other cofactors. The consumption of PMF may explain why DABs are typically only found in organisms that grow in low pH, where protons are abundant and CO_2 is the dominant species (Desmarais et al., 2019). Using alternative DIC transporters that do not consume PMF, such as SbtA or BicA, may be promising routes for a vectoral increase of cytosolic HCO_3^- in *C. necator,* and could lead to better autotrophic performance at scale compared to hnDAB2 or native Can CA.

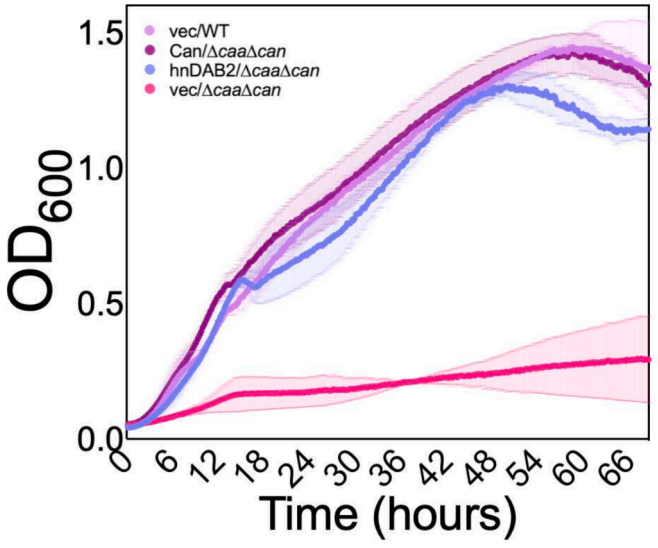

Fig. 4. DIC transporter hnDAB2 supports heterotrophic growth of the CA-defective strain in ambient air and 1% fructose minimal media. Error bars indicate the standard deviation of five technical replicates.

The data associated with the bioreactor experiments show a clear trend. However, we observed an anomalous growth stalling in the 5 % CO2 condition at 40 h, which may be associated with the bioreactor's pH maintenance protocol, as discussed in the supplementary information.

Chromosomal expression of hnDAB2 and heterologous rubisco expression

A plasmid-free system for expressing hnDAB2 would allow us to investigate the influence of heterologous rubisco expression in the context of DIC transport. To this end, the native genes for rubisco were deleted on chromosome 2, and pHG1 megaplasmid in the Δ*caa*Δ*can* strain to produce a strain with genotype Δ*caa*Δ*can*Δ*cbbLS2*Δ*cbbLSp,* and hnDAB2 was added to the chromosome by a modified version of the Chassis-independent Recombinase-Assisted Genome Engineering (CRAGE) technique (G. Wang et al., 2019). Briefly, a mariner transposon delivered a "landing pad" to the chromosome using a kanamycin selection. PacBio sequencing revealed that the landing pad landed in a 16S rRNA sequence, though no growth defects were observed in these strains. Next, a construct containing an expression cassette for hnDAB2 was delivered to the strain, and recombinants were selected for growth in ambient air (see supplementary information for details). The resulting strain (Δ*caa*Δ*can*Δ*cbbLS2*Δ*cbbLSp LP3::hndab2*) was used to assess the ability of rubisco homologs to recover autotrophic growth when paired with hnDAB2. We focused on bacterial rubisco homologs, as their requirements for assembly are well understood in

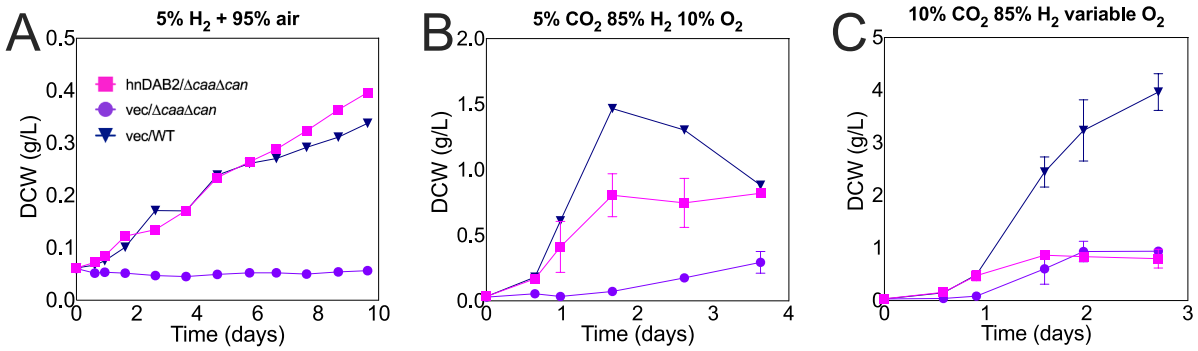

Fig. 5. Hndab2 restores growth of ca- strains to wt levels in ambient air in a continuously fed gas bioreactorsupplemented with 5 % H_2 but underperforms WT in 5 % and 10 % CO_2. The oxygen flow in bioreactors in panel B was gradually incremented from an initial value of 3 % over the total gas flow to maintain DO levels of approximately > 5 %. Note the differences in scale of the y-axes when comparing panels. The experiment in Panel C started with a flow of 3.5 % O_2 and 86.5 % H_2. Oxygen flow was adjusted as consumed to maintain dissolved oxygen saturation levels under 30 % to minimize any possible inhibition of autotrophic growth.

C. necator, and the kinetic profiles of tested rubisco homologs are described in Table 3. All rubisco homologs were cloned onto a pBBR1-MCS plasmid driven by a native *C. necator* cbb_R promoter. We found that the rubiscos from *R. rubrum* and *R. sphaeroides* worked best in our system, though the fastest known bacterial rubisco from *Gallionella* sp. failed to grow (Davidi et al., 2020) (Fig. 6). The expression of rubisco from *Synechococcus elongatus* PCC6301 did not rescue growth in *C. necator*, in agreement with previous findings (Satagopan and Tabita, 2016).

Completely rewired CO_2 and HCO_3^- metabolism.

We have shown that the CO_2/HCO_3^- circuit in *C. necator* can be manipulated by replacing the native CAs and rubiscos with heterologous systems, including the expression of three different types of bicarbonate transporters and the functional expression of several types of rubisco homologs. Given that the examined rubiscos were chosen based on exemplary kinetic profiles, it is perhaps unsurprising that the expression of hnDAB2 largely governed the ability of *C. necator* to grow in autotrophic conditions. We found that *C. necator* can assemble functional rubiscos from several subtypes and geometries, which could pave the path toward highly efficient autotrophic bioproduction strains. *C. necator* features a form IC rubisco with L_8S_8 geometry, though the best-performing heterologous rubisco was the *R. rubrum* rubisco, which is form II and has an L2 geometry. The rubisco from R. rubrum is phylogenetically distinct from the rubisco in *C. necator* and has a broadly different kinetic profile (Table 3) (Davidi et al., 2020; Satagopan and Tabita, 2016). Surprisingly, a rubisco variant from *Gallionella* sp. did not function in our strain despite having a similar kinetic profile to *R. rubrum* rubisco (Davidi et al., 2020). It is plausible that this variant's expression is weak or the protein is not correctly folded in *C. necator*. The gene was codon-optimized for expression in *E. coli* from a previous study. We have identified five UGU and five GUA codons in this gene, which are relatively rare in *C. necator* H16. This gene also has a GC content of 50.6 %, substantially lower than *C. necator's* GC content (~67 %).

Synthetic CO_2 metabolisms and heterologous CCM expression: progress toward increased crop yield.

Recently, there has been interest in optimizing carbon fixation pathways in organisms by expressing heterologous rubiscos or introducing CCMs, especially in crops, to increase food production. Our work is an important stepping stone for expressing a full CCM in *C. necator,* and we propose that our system is ideal for rapidly prototyping synthetic CO_2 fixation systems and CCMs for further engineering in plants (Durão et al., 2015; Lin et al., 2014; Whitney et al., 2015). In contrast, eukaryotic hosts and many cyanobacteria are difficult and time-consuming to engineer. On the other hand, common bacterial hosts such as *E. coli* are not appropriate for screening for autotrophic growth advantages (Mueller-Cajar and Whitney, 2008; Smith and Tabita, 2003; Spreitzer and Salvucci, 2002). Using an *E. coli* strain dependent on the detoxification of RuBP to screen active rubiscos often gives false positives (Flamholz et al., 2020). The work here and in Satagopan S et al. show the utility of using *C. necator* H16 for high-throughput *in vivo* screening of rubisco performance, as the current methodology for biochemical screening of rubisco performance *in vitro* is labor and time-intensive.

4. Conclusions

This work highlights the dual role that CO_2 and its conjugate base, HCO_3^-, have in *C. necator*'s metabolic network. We have demonstrated flexibility in *C. necator* autotrophic metabolism by the heterologous expression of bicarbonate acquisition systems and rubisco homologs. Our findings suggest that the primary role of Can during autotrophic growth is for bicarbonate accumulation, to be used as a cofactor by central metabolic enzymes, a function that DIC transporters can complement. We propose that *C. necator* is an ideal system for engineering novel CO_2 metabolisms, such as PEP-driven carboxylation cycles or

Table 3
Kinetic parameters of investigated rubisco homologs.

Organism	Form	Type	k_{cat} (s^{-1})	K_M (μM)	k_{cat}/K_M ($s^{-1}mM^{-1}$)	$S_{C/O}$	Reference
C. necator H16	IC	L_8S_8	3.84 +/- 0.54	37 +/- 4	104	75	1,2
R. rubrum	II	L_2	6.6 +/- 0.3	109 +/- 2	60	12.5	3
R. sphaeroides	IC	L_8S_8	6.7 +/- ND	36 +/- ND	186	62	3
S. elongatus PCC 6301	II	L_8S_8	11.4 +/- 0.6	273 +/- 10	42	43.9	4
Gallionella sp.	II	L_2	22.2 +/- 1.1	276 +/- 6	80	10	3

[1](Horken and Tabita 1999).
[2](Satagopan and Tabita 2016).
[3](Davidi et al. 2020).
[4](Greene et al. 2007).

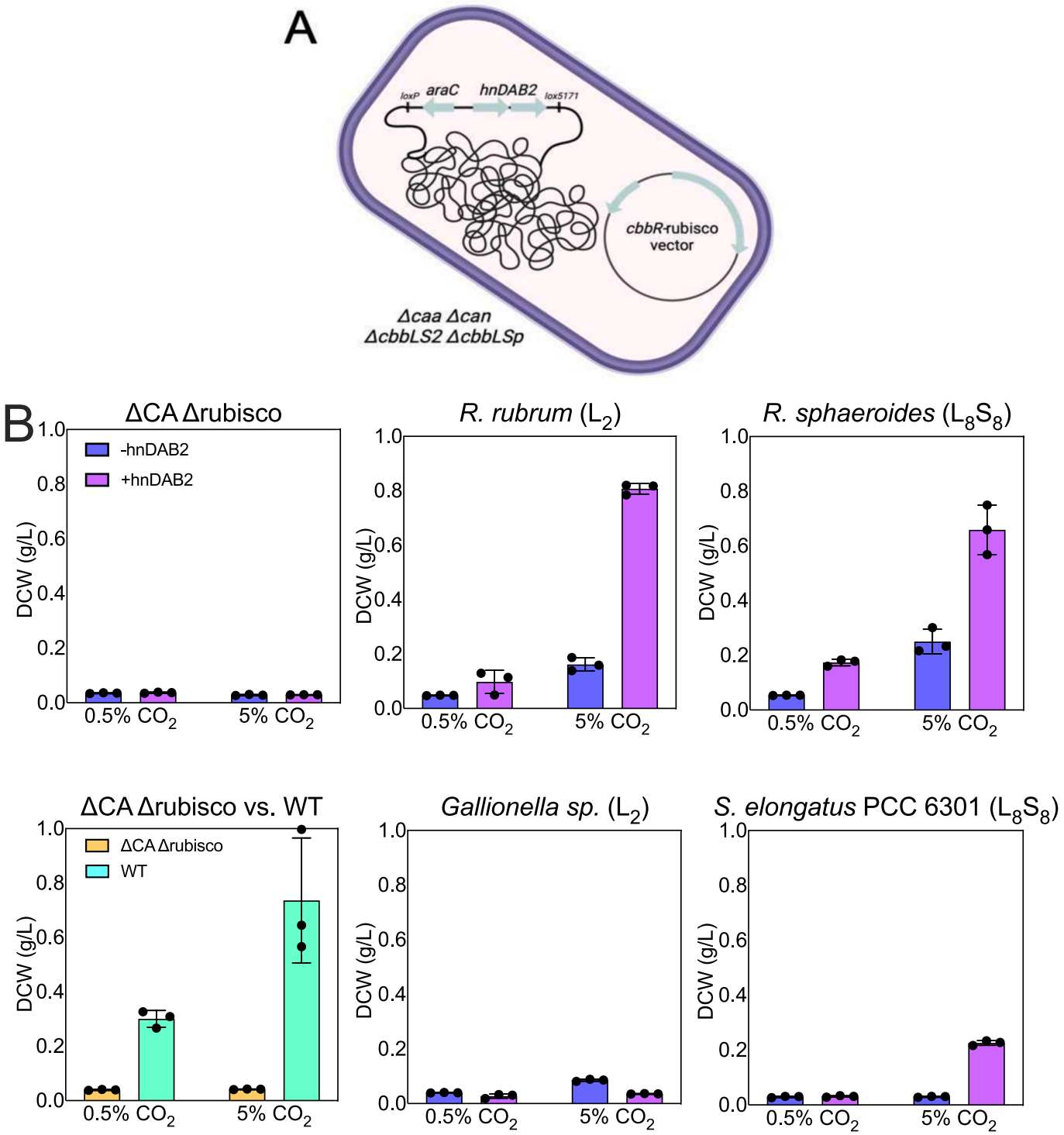

Fig. 6. Hndab2 activity improves growth in strains with heterologous rubisco expression. panel a) schematic describing the genetic configuration of strains used in these experiments. strains either had a landing pad harboring a kanamycin resistance cassette or hndab2 under an arabinose promoter integrated into the *rpsL* locus. Panel B) Terminal endpoints for autotrophic growth at 48 hr in strains heterologously expressing various rubisco homologs. Cells were inoculated at an OD_{600} of 0.10 from heterotrophic precultures in 62% H_2/10% O_2 and indicated CO_2. The source of the heterologous rubisco is indicated above each plot. Parentheses indicate the configuration of each rubisco in terms of large subunit (L) and small subunit (S) stoichiometry.

other pathways that are yet to be realized (Bar-Even et al., 2010; Schwander et al., 2016).

Funding

This work was supported by Shell International B.V (Energy & Biosciences Institute project CW163755 awarded to DFS and SWS and by the Advanced Biofuels and Bioproducts Process Development Unit (ABPDU) project, sponsored by the U.S. Department of Energy Bioenergy Technologies Office, under contract DEAC02-05CH11231 between DOE and Lawrence Berkeley National Laboratory. CRAGE development for *C. necator* was supported by the Laboratory Directed

Research and Development program at LBNL. The work conducted by the U.S. Department of Energy Joint Genome Institute (https://ror.org/04xm1d337), a DOE Office of Science User Facility, is supported by the Office of Science of the U.S. Department of Energy operated under Contract No. DE-AC02-05CH11231.

CRediT authorship contribution statement

Justin Panich: Writing – review & editing, Writing – original draft, Methodology, Investigation, Formal analysis, Data curation, Conceptualization. **Emili Toppari:** Investigation. **Sara Tejedor-Sanz:** Investigation, Data curation. **Bonnie Fong:** Investigation. **Eli Dugan:** Investigation. **Yan Chen:** Methodology, Investigation, Data curation. **Christopher J. Petzold:** Methodology. **Zhiying Zhao:** Methodology. **Yasuo Yoshikuni:** Methodology. **David F. Savage:** Writing – review & editing, Funding acquisition. **Steven W. Singer:** Supervision, Writing – review & editing, Funding acquisition.

Declaration of competing interest

The authors declare that they have no known competing financial interests or personal relationships that could have appeared to influence the work reported in this paper.

Data availability

Full datasets for proteomic and bioreactor experiments are available in the online supplement. Additional data will be made available upon request.

Acknowledgments

We thank Luke Oltrogge for his extensive and thoughtful comments on the manuscript.

and Eric Sundstrom for his mentorship regarding the gas bioreactor experiments.

Appendix A. Supplementary data

Supplementary data to this article can be found online at https://doi.org/10.1016/j.biortech.2024.131214.

References

Ahrné, E., Molzahn, L., Glatter, T., Schmidt, A., 2013. Critical assessment of proteome-wide label-free absolute abundance estimation strategies. Proteomics 13, 2567–2578. https://doi.org/10.1002/pmic.201300135.

Bar-Even, A., Noor, E., Lewis, N.E., Milo, R., 2010. Design and analysis of synthetic carbon fixation pathways. Proc Natl Acad Sci USA 107, 8889–8894. https://doi.org/10.1073/pnas.0907176107.

Bowien, B., Mayer, F., Codd, G.A., Schlegel, H.G., 1976. Purification, some properties and quaternary structure of the D-ribulose 1,5-diphosphate carboxylase of Alcaligenes eutrophus. Arch. Microbiol. 110, 157–166. https://doi.org/10.1007/BF00690223.

Calvey, C.H., Nogué, S.I., V., White, A.M., Kneucker, C.M., Woodworth, S.P., Alt, H.M., Eckert, C.A., Johnson, C.W, 2023. Improving growth of Cupriavidus necator H16 on formate using adaptive laboratory evolution-informed engineering. Metab. Eng. 75, 78–90. https://doi.org/10.1016/j.ymben.2022.10.016.

Chen, Y., Gin, J., Petzold, C.J., 2022. Discovery proteomic (DIA) LC-MS/MS data acquisition and analysis v2. dOI: 10.17504/protocols.io.e6nvwk1z7vmk/v2.

Chen, Y., Gin, J.W., Wang, Y., de Raad, M., Tan, S., Hillson, N.J., Northen, T.R., Adams, P.D., Petzold, C.J., 2023. Alkaline-SDS cell lysis of microbes with acetone protein precipitation for proteomic sample preparation in 96-well plate format. PLoS ONE 18, e0288102.

Claassens, N.J., Scarinci, G., Fischer, A., Flamholz, A.I., Newell, W., Frielingsdorf, S., Lenz, O., Bar-Even, A., 2020. Phosphoglycolate salvage in a chemolithoautotroph using the Calvin cycle. Proc Natl Acad Sci USA 117, 22452–22461. https://doi.org/10.1073/pnas.2012288117.

Davidi, D., Shamshoum, M., Guo, Z., Bar-On, Y.M., Prywes, N., Oz, A., Jablonska, J., Flamholz, A., Wernick, D.G., Antonovsky, N., de Pins, B., Shachar, L., Hochhauser, D., Peleg, Y., Albeck, S., Sharon, I., Mueller-Cajar, O., Milo, R., 2020. Highly active rubiscos discovered by systematic interrogation of natural sequence diversity. EMBO J. 39, e104081.

Demichev, V., Messner, C.B., Vernardis, S.I., Lilley, K.S., Ralser, M., 2020. DIA-NN: neural networks and interference correction enable deep proteome coverage in high throughput. Nat. Methods 17, 41–44. https://doi.org/10.1038/s41592-019-0638-x.

Desmarais, J.J., Flamholz, A.I., Blikstad, C., Dugan, E.J., Laughlin, T.G., Oltrogge, L.M., Chen, A.W., Wetmore, K., Diamond, S., Wang, J.Y., Savage, D.F., 2019. DABs are inorganic carbon pumps found throughout prokaryotic phyla. Nat. Microbiol. 4, 2204–2215. https://doi.org/10.1038/s41564-019-0520-8.

Du, J., Förster, B., Rourke, L., Howitt, S.M., Price, G.D., 2014. Characterisation of cyanobacterial bicarbonate transporters in E. coli shows that SbtA homologs are functional in this heterologous expression system. PLoS ONE 9, e115905.

Durão, P., Aigner, H., Nagy, P., Mueller-Cajar, O., Hartl, F.U., Hayer-Hartl, M., 2015. Opposing effects of folding and assembly chaperones on evolvability of Rubisco. Nat. Chem. Biol. 11, 148–155. https://doi.org/10.1038/nchembio.1715.

Espie, G.S., Kimber, M.S., 2011. Carboxysomes: cyanobacterial RubisCO comes in small packages. Photosyn. Res. 109, 7–20. https://doi.org/10.1007/s11120-011-9656-y.

Fan, S.-H., Matsuo, M., Huang, L., Tribelli, P.M., Götz, F., 2021. The MpsAB Bicarbonate Transporter Is Superior to Carbonic Anhydrase in Biofilm-Forming Bacteria with Limited CO2 Diffusion. Microbiol. Spectr. 9, e0030521.

Fang, S., Huang, X., Zhang, X., Zhang, M., Hao, Y., Guo, H., Liu, L.-N., Yu, F., Zhang, P., 2021. Molecular mechanism underlying transport and allosteric inhibition of bicarbonate transporter SbtA. Proc Natl Acad Sci USA 118. https://doi.org/10.1073/pnas.2101632118.

Flamholz, A.I., Dugan, E., Blikstad, C., Gleizer, S., Ben-Nissan, R., Amram, S., Antonovsky, N., Ravishankar, S., Noor, E., Bar-Even, A., Milo, R., Savage, D.F., 2020. Functional reconstitution of a bacterial CO2 concentrating mechanism in Escherichia coli. eLife 9. dOI: 10.7554/eLife.59882.

Flamholz, A.I., Dugan, E., Panich, J., Desmarais, J.J., Oltrogge, L.M., Fischer, W.W., Singer, S.W., Savage, D.F., 2022. Trajectories for the evolution of bacterial CO2-concentrating mechanisms. Proc Natl Acad Sci USA 119, e2210539119. dOI: 10.1073/pnas.2210539119.

Flamholz, A.I., Prywes, N., Moran, U., Davidi, D., Bar-On, Y.M., Oltrogge, L.M., Alves, R., Savage, D., Milo, R., 2019. Revisiting Trade-offs between Rubisco Kinetic Parameters. Biochemistry 58, 3365–3376. https://doi.org/10.1021/acs.biochem.9b00237.

Gai, C.S., Lu, J., Brigham, C.J., Bernardi, A.C., Sinskey, A.J., 2014. Insights into bacterial CO2 metabolism revealed by the characterization of four carbonic anhydrases in Ralstonia eutropha H16. AMB Express 4, 2. https://doi.org/10.1186/2191-0855-4-2.

Gascoyne, J.L., Bommareddy, R.R., Heeb, S., Malys, N., 2021. Engineering Cupriavidus necator H16 for the autotrophic production of (R)-1,3-butanediol. Metab. Eng. 67, 262–276. https://doi.org/10.1016/j.ymben.2021.06.010.

Greene, D.N., Whitney, S.M., Matsumura, I., 2007. Artificially evolved Synechococcus PCC6301 Rubisco variants exhibit improvements in folding and catalytic efficiency. Biochem. J. 404, 517–524. https://doi.org/10.1042/BJ20070071.

Gupta, J.K., Rai, P., Jain, K.K., Srivastava, S., 2020. Overexpression of bicarbonate transporters in the marine cyanobacterium Synechococcus sp. PCC 7002 increases growth rate and glycogen accumulation. Biotechnol. Biofuels 13, 17. https://doi.org/10.1186/s13068-020-1656-8.

Gutknecht, J., Bisson, M.A., Tosteson, F.C., 1977. Diffusion of carbon dioxide through lipid bilayer membranes: effects of carbonic anhydrase, bicarbonate, and unstirred layers. J. Gen. Physiol. 69, 779–794. https://doi.org/10.1085/jgp.69.6.779.

Han, X., Sun, N., Xu, M., Mi, H., 2017. Co-ordination of NDH and Cup proteins in CO2 uptake in cyanobacterium Synechocystis sp. PCC 6803. J. Exp. Bot. 68, 3869–3877. https://doi.org/10.1093/jxb/erx129.

Hannesschlaeger, C., Horner, A., Pohl, P., 2019. Intrinsic membrane permeability to small molecules. Chem. Rev. 119, 5922–5953. https://doi.org/10.1021/acs.chemrev.8b00560.

Hashimoto, M., Kato, J., 2003. Indispensability of the Escherichia coli carbonic anhydrases YadF and CynT in cell proliferation at a low CO2 partial pressure. Biosci. Biotechnol. Biochem. 67, 919–922. https://doi.org/10.1271/bbb.67.919.

He, Q., Silliman, B.R., 2019. Climate change, human impacts, and coastal ecosystems in the anthropocene. Curr. Biol. 29, R1021–R1035. https://doi.org/10.1016/j.cub.2019.08.042.

Hines, K.M., Chaudhari, V., Edgeworth, K.N., Owens, T.G., Hanson, M.R., 2021. Absence of carbonic anhydrase in chloroplasts affects C3 plant development but not photosynthesis. Proc Natl Acad Sci USA 118. https://doi.org/10.1073/pnas.2107425118.

Horken, K.M., Tabita, F.R., 1999. Closely related form I ribulose bisphosphate carboxylase/oxygenase molecules that possess different CO2/O2 substrate specificities. Arch. Biochem. Biophys. 361, 183–194. https://doi.org/10.1006/abbi.1998.0979.

Iizasa, E., Nagano, Y., 2006. Highly efficient yeast-based in vivo DNA cloning of multiple DNA fragments and the simultaneous construction of yeast/ Escherichia coli shuttle vectors. BioTechniques 40, 79–83. https://doi.org/10.2144/000112041.

Jahn, M., Crang, N., Janasch, M., Hober, A., Forsström, B., Kimler, K., Mattausch, A., Chen, Q., Asplund-Samuelsson, J., Hudson, E.P., 2021. Protein allocation and utilization in the versatile chemolithoautotroph Cupriavidus necator. eLife 10. dOI: 10.7554/eLife.69019.

Koch, M., Bowes, G., Ross, C., Zhang, X.-H., 2013. Climate change and ocean acidification effects on seagrasses and marine macroalgae. Glob. Chang. Biol. 19, 103–132. https://doi.org/10.1111/j.1365-2486.2012.02791.x.

Kusian, B., Sültemeyer, D., Bowien, B., 2002. Carbonic anhydrase is essential for growth of Ralstonia eutropha at ambient CO(2) concentrations. J. Bacteriol. 184, 5018–5026. https://doi.org/10.1128/JB.184.18.5018-5026.2002.

Lin, M.T., Occhialini, A., Andralojc, P.J., Parry, M.A.J., Hanson, M.R., 2014. A faster Rubisco with potential to increase photosynthesis in crops. Nature 513, 547–550. https://doi.org/10.1038/nature13776.

Liu, Z., Deng, Z., Davis, S., Ciais, P., 2023. Monitoring global carbon emissions in 2022. Nat. Rev. Earth Environ. 4, 205–206. https://doi.org/10.1038/s43017-023-00406-z.

Löwe, H., Beentjes, M., Pflüger-Grau, K., Kremling, A., 2021. Trehalose production by Cupriavidus necator from CO2 and hydrogen gas. Bioresour. Technol. 319, 124169 https://doi.org/10.1016/j.biortech.2020.124169.

Mangan, N.M., Flamholz, A., Hood, R.D., Milo, R., Savage, D.F., 2016. pH determines the energetic efficiency of the cyanobacterial CO2 concentrating mechanism. Proc Natl Acad Sci USA 113, E5354–E5362. https://doi.org/10.1073/pnas.1525145113.

Mangiapia, M., USF MCB4404L, Brown, T.-R.W., Chaput, D., Haller, E., Harmer, T.L., Hashemy, Z., Keeley, R., Leonard, J., Mancera, P., Nicholson, D., Stevens, S., Wanjugi, P., Zabinski, T., Pan, C., Scott, K.M, 2017. Proteomic and Mutant Analysis of the CO2 Concentrating Mechanism of Hydrothermal Vent Chemolithoautotroph Thiomicrospira crunogena. J. Bacteriol. 199 https://doi.org/10.1128/JB.00871-16.

Merlin, C., Masters, M., McAteer, S., Coulson, A., 2003. Why is carbonic anhydrase essential to Escherichia coli? J. Bacteriol. 185, 6415–6424. https://doi.org/10.1128/JB.185.21.6415-6424.2003.

Milker, S., Holtmann, D., 2021. First time β-farnesene production by the versatile bacterium Cupriavidus necator. Microb. Cell Fact. 20, 89. https://doi.org/10.1186/s12934-021-01562-x.

Milker, S., Sydow, A., Torres-Monroy, I., Jach, G., Faust, F., Kranz, L., Tkatschuk, L., Holtmann, D., 2021. Gram-scale production of the sesquiterpene α-humulene with Cupriavidus necator. Biotechnol. Bioeng. 118, 2694–2702. https://doi.org/10.1002/bit.27788.

Mitsuhashi, S., Ohnishi, J., Hayashi, M., Ikeda, M., 2004. A gene homologous to beta-type carbonic anhydrase is essential for the growth of Corynebacterium glutamicum under atmospheric conditions. Appl. Microbiol. Biotechnol. 63, 592–601. https://doi.org/10.1007/s00253-003-1402-8.

Mueller-Cajar, O., Whitney, S.M., 2008. Directing the evolution of Rubisco and Rubisco activase: first impressions of a new tool for photosynthesis research. Photosyn. Res. 98, 667–675. https://doi.org/10.1007/s11120-008-9324-z.

Nangle, S.N., Ziesack, M., Buckley, S., Trivedi, D., Loh, D.M., Nocera, D.G., Silver, P.A., 2020. Valorization of CO2 through lithoautotrophic production of sustainable chemicals in Cupriavidus necator. Metab. Eng. 62, 207–220. https://doi.org/10.1016/j.ymben.2020.09.002.

Oecd, 2023. CO2 emissions in 2022. OECD. https://doi.org/10.1787/12ad1e1a-en.

Omata, T., Takahashi, Y., Yamaguchi, O., Nishimura, T., 2002. Structure, function and regulation of the cyanobacterial high-affinity bicarbonate transporter, BCT1. Funct. Plant Biol. 29, 151–159. https://doi.org/10.1071/PP01215.

Panich, J., Fong, B., Singer, S.W., 2021. Metabolic Engineering of Cupriavidus necator H16 for Sustainable Biofuels from CO2. Trends Biotechnol. 39, 412–424. https://doi.org/10.1016/j.tibtech.2021.01.001.

Perez-Riverol, Y., Bai, J., Bandla, C., García-Seisdedos, D., Hewapathirana, S., Kamatchinathan, S., Kundu, D.J., Prakash, A., Frericks-Zipper, A., Eisenacher, M., Walzer, M., Wang, S., Brazma, A., Vizcaíno, J.A., 2022. The PRIDE database resources in 2022: a hub for mass spectrometry-based proteomics evidences. Nucleic Acids Res. 50, D543–D552. https://doi.org/10.1093/nar/gkab1038.

Salinas, A., McGregor, C., Irorere, V., Arenas-López, C., Bommareddy, R.R., Winzer, K., Minton, N.P., Kovács, K., 2022. Metabolic engineering of Cupriavidus necator H16 for heterotrophic and autotrophic production of 3-hydroxypropionic acid. Metab. Eng. 74, 178–190. https://doi.org/10.1016/j.ymben.2022.10.014.

Satagopan, S., Tabita, F.R., 2016. RubisCO selection using the vigorously aerobic and metabolically versatile bacterium Ralstonia eutropha. FEBS J. 283, 2869–2880. https://doi.org/10.1111/febs.13774.

Schwander, T., Schada von Borzyskowski, L., Burgener, S., Cortina, N.S., Erb, T.J., 2016. A synthetic pathway for the fixation of carbon dioxide in vitro. Science 354, 900–904. https://doi.org/10.1126/science.aah5237.

Scott, K.M., Leonard, J.M., Boden, R., Chaput, D., Dennison, C., Haller, E., Harmer, T.L., Anderson, A., Arnold, T., Budenstein, S., Brown, R., Brand, J., Byers, J., Calarco, J., Campbell, T., Carter, E., Chase, M., Cole, M., Dwyer, D., Grasham, J., Hanni, C., Hazle, A., Johnson, C., Johnson, R., Kirby, B., Lewis, K., Neumann, B., Nguyen, T., Nino Charari, J., Morakinyo, O., Olsson, B., Roundtree, S., Skjerve, E., Ubaldini, A., Whittaker, R., 2019. Diversity in CO2-Concentrating Mechanisms among Chemolithoautotrophs from the Genera Hydrogenovibrio, Thiomicrorhabdus, and Thiomicrospira, Ubiquitous in Sulfidic Habitats Worldwide. Appl. Environ. Microbiol. 85 https://doi.org/10.1128/AEM.02096-18.

Shibata, M., Katoh, H., Sonoda, M., Ohkawa, H., Shimoyama, M., Fukuzawa, H., Kaplan, A., Ogawa, T., 2002. Genes essential to sodium-dependent bicarbonate transport in cyanobacteria: function and phylogenetic analysis. J. Biol. Chem. 277, 18658–18664. https://doi.org/10.1074/jbc.M112468200.

Silva, J.C., Gorenstein, M.V., Li, G.-Z., Vissers, J.P.C., Geromanos, S.J., 2006. Absolute quantification of proteins by LCMSE: a virtue of parallel MS acquisition. Mol. Cell. Proteomics 5, 144–156. https://doi.org/10.1074/mcp.M500230-MCP200.

Smith, S.A., Tabita, F.R., 2003. Positive and negative selection of mutant forms of prokaryotic (cyanobacterial) ribulose-1,5-bisphosphate carboxylase/oxygenase. J. Mol. Biol. 331, 557–569. https://doi.org/10.1016/s0022-2836(03)00786-1.

Sohn, Y.J., Son, J., Jo, S.Y., Park, S.Y., Yoo, J.I., Baritugo, K.-A., Na, J.G., Choi, J.-I., Kim, H.T., Joo, J.C., Park, S.J., 2021. Chemoautotroph Cupriavidus necator as a potential game-changer for global warming and plastic waste problem: A review. Bioresour. Technol. 340, 125693 https://doi.org/10.1016/j.biortech.2021.125693.

Spreitzer, R.J., Salvucci, M.E., 2002. Rubisco: structure, regulatory interactions, and possibilities for a better enzyme. Annu. Rev. Plant Biol. 53, 449–475. https://doi.org/10.1146/annurev.arplant.53.100301.135233.

van Leeuwen, J., Andrews, B., Boone, C., Tan, G., 2015. Construction of multifragment plasmids by homologous recombination in yeast. Cold Spring Harb. Protoc. 2015, pdb.top084111. dOI: 10.1101/pdb.top084111.

Wang, X., Luo, H., Wang, Y., Wang, Y., Tu, T., Qin, X., Su, X., Huang, H., Bai, Y., Yao, B., Zhang, J., 2022. Direct conversion of carbon dioxide to glucose using metabolically engineered Cupriavidus necator. Bioresour. Technol. 362, 127806 https://doi.org/10.1016/j.biortech.2022.127806.

Wang, C., Sun, B., Zhang, X., Huang, X., Zhang, M., Guo, H., Chen, X., Huang, F., Chen, T., Mi, H., Yu, F., Liu, L.-N., Zhang, P., 2019a. Structural mechanism of the active bicarbonate transporter from cyanobacteria. Nat. Plants 5, 1184–1193. https://doi.org/10.1038/s41477-019-0538-1.

Wang, X., Wang, K., Wang, L., Luo, H., Wang, Y., Wang, Y., Tu, T., Qin, X., Su, X., Bai, Y., Yao, B., Huang, H., Zhang, J., 2023. Engineering Cupriavidus necator H16 for heterotrophic and autotrophic production of myo-inositol. Bioresour. Technol. 368, 128321 https://doi.org/10.1016/j.biortech.2022.128321.

Wang, G., Zhao, Z., Ke, J., Engel, Y., Shi, Y.-M., Robinson, D., Bingol, K., Zhang, Z., Bowen, B., Louie, K., Wang, B., Evans, R., Miyamoto, Y., Cheng, K., Kosina, S., De Raad, M., Silva, L., Luhrs, A., Lubbe, A., Hoyt, D.W., Francavilla, C., Otani, H., Deutsch, S., Washton, N.M., Rubin, E.M., Mouncey, N.J., Visel, A., Northen, T., Cheng, J.-F., Bode, H.B., Yoshikuni, Y., 2019b. CRAGE enables rapid activation of biosynthetic gene clusters in undomesticated bacteria. Nat. Microbiol. 4, 2498–2510. https://doi.org/10.1038/s41564-019-0573-8.

Whitney, S.M., Birch, R., Kelso, C., Beck, J.L., Kapralov, M.V., 2015. Improving recombinant Rubisco biogenesis, plant photosynthesis and growth by coexpressing its ancillary RAF1 chaperone. Proc Natl Acad Sci USA 112, 3564–3569. https://doi.org/10.1073/pnas.1420536112.

Yu, J., Munasinghe, P., 2018. Gas Fermentation Enhancement for Chemolithotrophic Growth of Cupriavidus necator on Carbon Dioxide. Fermentation 4, 63. https://doi.org/10.3390/fermentation4030063.

Zhou, Y., Whitney, S., 2019. Directed Evolution of an Improved Rubisco; In Vitro Analyses to Decipher Fact from Fiction. Int. J. Mol. Sci. 20 https://doi.org/10.3390/ijms20205019.